

The influence of Cr alloying on microstructures of Fe–Al–Mn–Cr alloys

J.W. Lee ^{a,*}, C.C. Wu ^b, T.F. Liu ^a

^a Department of Materials Science and Engineering, National Chiao Tung University, 1001 Ta Hsueh Road, 300 Hsinchu, Taiwan, Republic of China

^b Department of Mechanical Engineering, Southern Taiwan University of Technology, Tainan, Taiwan, Republic of China

Received 3 November 2003; received in revised form 23 February 2004; accepted 25 February 2004

Abstract

The effects of increasing chromium content on the phase transformations in Fe–Al–Mn–Cr alloys have been investigated by means of transmission electron microscopy and energy-dispersive X-ray spectrometry. The experimental results revealed that increasing the chromium addition would expand both the A12 α -Mn and DO₃ phase-field regions.

© 2004 Acta Materialia Inc. Published by Elsevier Ltd. All rights reserved.

Keywords: Fe–Al–Mn–Cr alloys; Phase transformations; TEM; Aging; Precipitation

1. Introduction

For economic and strategic considerations, Fe–Al–Mn alloys with aluminum and manganese as substitutes for chromium and nickel used in conventional stainless steels have been widely investigated by many workers [1–3]. On the basis of their studies, it is generally concluded that the Fe–Al–Mn alloys possess a good oxidation resistance at high temperatures; however, the corrosion resistance of the Fe–Al–Mn alloys was inferior to that of the conventional stainless steels. It was reported that the addition of chromium to the Fe–Al–Mn alloys could significantly improve the corrosion resistance [4,5]. Additionally, iron aluminides also attracted much interest due to their superior characteristics at high temperature. But, applications have been restricted by their embrittlement at ambient temperature. So far, chromium was found to be the most effective alloying element to improve their environmental embrittlement [6,7]. One possible reason that has been proposed is that alloying of chromium into Fe–Al alloys would suppress the formation of the brittle ordered DO₃ phase. However, up to now, little information concerning the microstructures of the Fe–Al–Mn–Cr alloys

has been reported. We first performed transformation electron microscopy observations on the phase transformations of an Fe–9.1wt.%Al–29.9wt.%Mn–2.9wt.%Cr alloy [8–10]. Based on our previous studies, the phase transformation sequence of the Fe–9.1Al–29.9Mn–2.9Cr alloy with increasing aging temperature was found to be (ferrite + DO₃) + austenite → (ferrite + DO₃ + A12 α -Mn) + austenite → (ferrite + A12 α -Mn) + austenite → (ferrite + A13 β -Mn) + austenite → ferrite + austenite, in which the transitions occurred at temperatures between 410 and 430 °C, 450 and 500 °C, 520 and 550 °C and 800 and 850 °C in sequence. Extending the previous work, it is interesting to study successively the effects of the higher chromium contents on the microstructural developments of Fe–Al–Mn–Cr alloys. Therefore, the purpose of this work is an attempt to examine the microstructural developments of both the Fe–8.0Al–29.7Mn–5.0Cr and Fe–8.1Al–29.8Mn–10.0Cr alloys aged at temperatures ranging from 350 to 850 °C.

2. Experimental procedure

Two alloys of compositions Fe–8.0wt.%Al–29.7wt.%Mn–5.0wt.%Cr (designated as 5Cr) and Fe–8.1wt.%Al–29.8wt.%Mn–10.0wt.%Cr (designated as 10Cr) alloys were prepared in a vacuum induction furnace. In addition to contain 5.0 and 10 wt.% chromium, respectively,

* Corresponding author. Tel.: +88-63-571-2121x55363; fax: +88-63-571-3987.

E-mail address: davidlee@cc.nctu.edu.tw (J.W. Lee).

both the alloys were composed of similar compositions. After being homogenized, slices sectioned from the ingots were subsequently solution heat-treated at 1050 °C for 2 h and then quenched into room temperature water. The aging processes were performed at temperatures ranging from 350 to 850 °C for various times in a vacuum heat-treatment furnace. Electron microscopy was performed on a JEOL-2000FX scanning transmission electron microscopy operating at 200 kV. This microscope was equipped with a Link ISIS 300 energy-dispersive X-ray spectrometer (EDS) for chemical analysis.

3. Results and discussion

Optical microscopy examinations exhibited that the as-quenched microstructure of the 5Cr alloy was the mixture of the continuous ferrite (α) phase and the discrete austenite (γ) phase, which is similar to that of the Fe–9.1Al–29.9Mn–2.9Cr alloy in our previous study [8]. As the chromium content was increased from 5 to 10 wt.%, the as-quenched microstructure of the 10Cr alloy was changed from duplex ($\alpha + \gamma$) phases to single α phase. Transmission electron microscopy examinations also indicated that when the as-quenched 5Cr alloy was heat-treated by subsequent aging processes, no precipitates were ever found within the austenite phase. Therefore, besides the phase transformations in the 10Cr alloy, only the microstructural changes inside the ferrite grains in the 5Cr alloy are discussed in the present study.

Fig. 1(a) is a bright-field (BF) electron micrograph of the 10Cr alloy aged at 350 °C for 2 h, revealing that fine precipitates were formed within the interior ferrite grain;

moreover, not only fine precipitates but also some irregular-shaped precipitates could be observed along grain boundary. Fig. 1(b), a selected-area diffraction pattern (SADP) taken from the mixed region covering the fine precipitates and the surrounding ferrite matrix in Fig. 1(a) indicates that the fine precipitates have an ordered DO_3 structure with lattice parameter $a = 0.578$ nm. Fig. 1(c) is a SADP taken from an area covering fine precipitates and irregularly shaped precipitates formed on the grain boundary in Fig. 1(a). As compared to Fig. 1(b), in addition to the ordered DO_3 phase, another kind of precipitate could also be detected. From analyzing this SADP, the lattice parameter of the other precipitate was determined to be of 0.888 nm and the orientation relationship between the precipitate and the ferrite matrix was cubic to cubic. Compared with our previous study in the Fe–9.1Al–29.9Mn–2.9Cr alloy [9], the precipitates are of $\text{Al}_2\alpha\text{-Mn}$ with a complex bcc structure. Fig. 1(d) is a $(111)\text{DO}_3$ dark-field (DF) electron micrograph, demonstrating that fine DO_3 precipitates were formed not only within the interior ferrite grain but also along grain boundary. However, the $(011)\alpha\text{-Mn}$ DF electron micrograph shows that these irregularly shaped $\alpha\text{-Mn}$ precipitates were only formed along grain boundary, as illustrated in Fig. 1(e). With progressing aging time at the same temperature, no evidence of other precipitates than that of the DO_3 phase and the $\alpha\text{-Mn}$ could be found. Fig. 2(a) and (b) is the $(111)\text{DO}_3$ and $(011)\alpha\text{-Mn}$ DF electron micrographs indicating that in addition to grown DO_3 particles, $\alpha\text{-Mn}$ precipitates started to appear inside the ferrite grains. After prolonged aging time to reach equilibrium condition at 350 °C, the microstructure of the alloy was still a mixture of

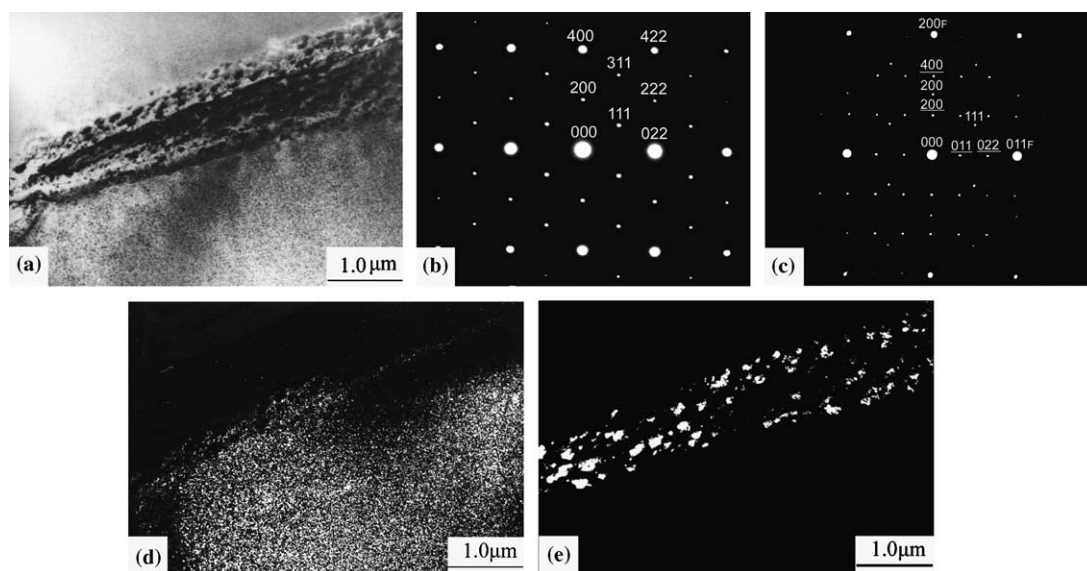


Fig. 1. Electron micrographs of the 10Cr alloy aged at 350 °C for 2 h: (a) BF; (b) and (c) two SADPs taken from the ferrite grain interior and grain boundary in (a), respectively. The zone axes are $[01\bar{1}]$. (hkl_F = ferrite, hkl = DO_3 phase, hkl = $\alpha\text{-Mn}$) (d) and (e) are $(111)\text{DO}_3$ and $(011)\alpha\text{-Mn}$ DF, respectively.

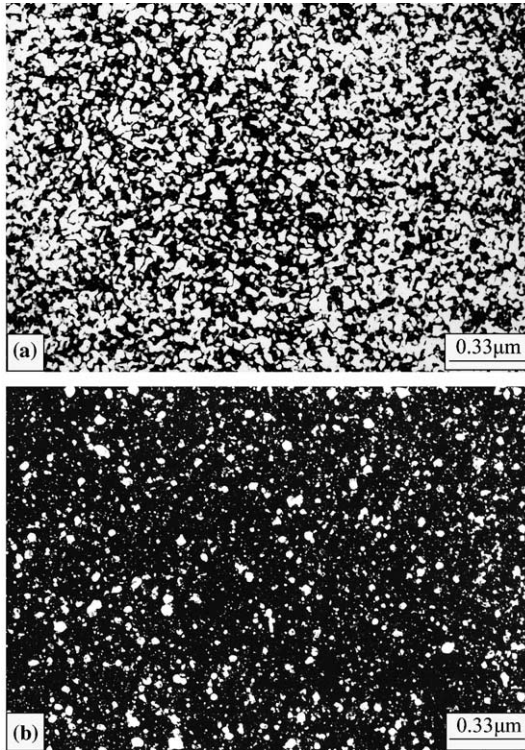


Fig. 2. Electron micrographs of the 10Cr alloy aged at 350 °C for 240 h: (a) (1 1 1)DO₃ DF, and (b) (0 1 1)α-Mn DF.

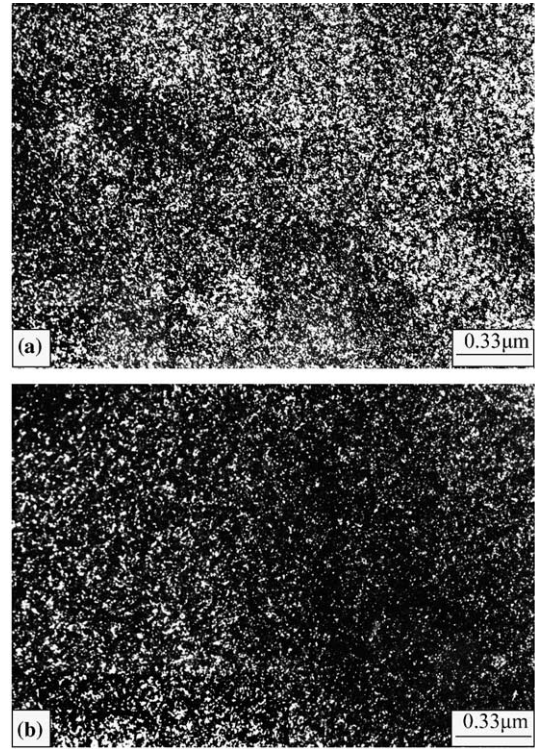


Fig. 3. Electron micrographs of the 10Cr alloy aged at 450 °C for 1 h: (a) (1 1 1)DO₃ DF and (b) (0 1 1)α-Mn DF.

(α + DO₃ + α-Mn) phases. Transmission electron microscopy examinations also revealed that the microstructural change within the ferrite grains in the 5Cr alloy aged at 350 °C was similar to that in the 10Cr alloy. However, this result is different from that reported by the present workers in the Fe–9.1Al–29.9Mn–2.9Cr alloy, in which only DO₃ phase was observed within the ferrite matrix at aging temperatures ranging from 350 to 410 °C [8].

Fig. 3(a) and (b) is the (1 1 1)DO₃ and (0 1 1)α-Mn DF electron micrographs of the 10Cr alloy aged at 450 °C for short time, revealing that the extremely fine DO₃ and α-Mn precipitates were formed almost simultaneously within the ferrite matrix. When the 10Cr alloy was aged at 450 °C for 48 h, the DO₃ and α-Mn precipitates have grown in shapes of sphere and polygon, respectively, as shown in Fig. 4(a) and (b). Moreover, it is clearly seen in Fig. 4(a) that the DO₃ phase was also formed at regions surrounding the polygonal-shaped α-Mn precipitates. It is demonstrated that at the aging temperature of 450 °C, the microstructure of the 5Cr alloy was similar to that of the 10Cr alloy, but the amount of the DO₃ phase in Fig. 5 was obviously less than that in Fig. 4(a).

When the 10Cr alloy was aged at 550 °C for short time, in addition to the α-Mn precipitates, no evidence of the DO₃ phase could be found within the ferrite grains, as shown in Fig. 6(a), a BF electron micrograph. By contrast, the α-Mn precipitates were formed more

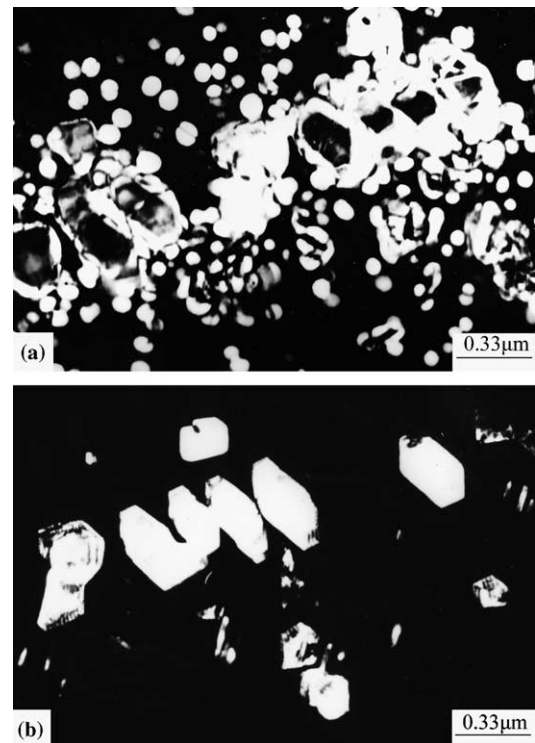


Fig. 4. Electron micrographs of the 10Cr alloy aged at 450 °C for 48 h: (a) (1 1 1)DO₃ DF and (b) (0 1 1)α-Mn DF.

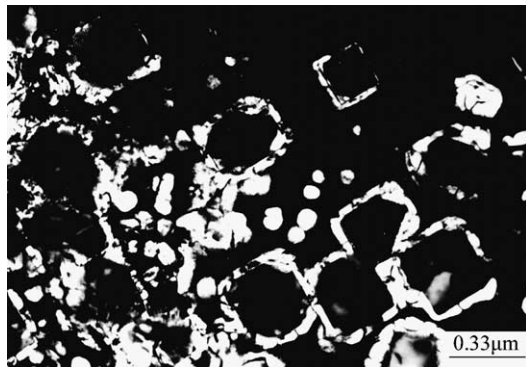


Fig. 5. (111)DO₃ DF electron micrograph of the 5Cr alloy aged at 450 °C for 48 h.

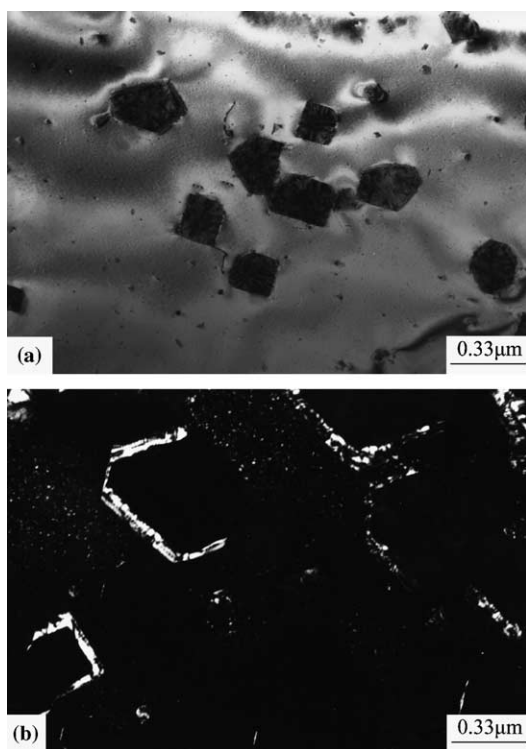


Fig. 6. Electron micrographs of the 10Cr alloy aged at 550 °C: (a) BF, after 2 h and (b) (111)DO₃ DF, after 24 h.

rapidly inside the internal ferrite grains at a temperature higher than 350 °C (i.e. 450, 550 °C). After being aged at 550 °C for 24 h, it is clearly demonstrated in Fig. 6(b) that the DO₃ phase would be formed not only within the ferrite grains but also around the α -Mn precipitates. Nevertheless, it is apparent that the amount of the DO₃ phase in Fig. 6(b) is much less than that in Fig. 4(a). On the contrary, even though the 5Cr was aged at 550 °C for a long period of time, in addition to the presence of well-grown α -Mn precipitates, the DO₃ phase could be detected neither within the ferrite grains nor around the periphery of the α -Mn precipitates. Transmission electron microscopy examinations revealed that the DO₃

phase existing in the 10Cr alloy could not be observed above 600 °C and the microstructure in equilibrium stage at 650 °C was a mixture of ($\alpha + \alpha$ -Mn) phases, which could be preserved up to a temperature between 700 and 750 °C. In the 5Cr alloy; however, the ($\alpha + \alpha$ -Mn) phases could only be maintained up to a lower temperature between 600 and 650 °C. When the 10Cr and 5Cr alloys were aged at temperatures above the existing temperatures of ($\alpha + \alpha$ -Mn) phases, namely 750 and 650 °C, respectively, another kind of precipitate with Widmanstätten morphology could be observed within the ferrite matrix in both the alloys. A typical example is shown in Fig. 7(a). Fig. 7(b) is an SADP taken from an area covering the needle-like precipitate and its surrounding ferrite matrix in Fig. 7(a), indicating that the precipitates with Widmanstätten morphology are of A13 β -Mn having a simple cubic structure with lattice parameter $a = 0.630$ nm [10]. Transmission electron microscopy examinations also exhibited that the stable microstructure of ($\alpha + \beta$ -Mn) phases in both the alloys could be observed at aging temperature up to somewhere between 800 and 850 °C. However, when both the alloys were aged at temperatures above 850 °C, no evidence of any precipitate could be detected within the ferrite grains. This feature is consistent with that observed in both the as-quenched alloys.

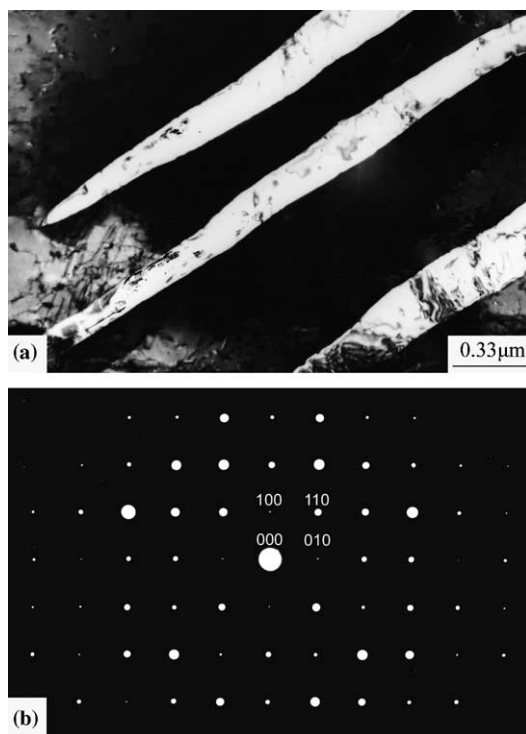


Fig. 7. Electron micrographs of the 10Cr alloy aged at 750 °C for 6 h: (a) BF; (b) an SADP taken from an area covering the needle-like precipitate and its surrounding ferrite matrix in (a). The zone axis is [001]. ($hkl = \beta$ -Mn.)

Based on the above observations, some experimental results are discussed below. When the two present alloys containing 5.0 and 10 wt.% chromium were aged at 350 °C, the stable microstructure was a mixture of (α + DO₃ + α -Mn) phases, rather than (α + DO₃) phases as observed in the Fe–9.1Al–29.9Mn–2.9Cr alloy aged in the temperature range 350–410 °C in our previous study [8]. Comparing the present 10Cr and 5Cr alloys with the previous Fe–9.1Al–29.9Mn–2.9Cr alloys, it is also worthwhile to note that not only the α -Mn but also the DO₃ phase could be preserved up to higher temperatures in the alloy containing a higher chromium content [9]. Conversely, it was reported that alloying of chromium into Fe–Al alloys would suppress the formation of the DO₃ phase so that the environment embrittlement of Fe–Al alloys would be reduced [6]. In order to clarify these features, a STEM-EDS study was performed. The quantitative analyses of at least 10 different EDS profiles exhibited that the average chemical composition of the α -Mn in the 10Cr alloy aged at 450 °C was Fe–(4.3 ± 0.4)Al–(41.2 ± 0.3)Mn–(20.1 ± 0.5)Cr (percent by weight). It is obviously seen that not only the manganese but also the chromium content of the α -Mn is much greater than that of the ferrite matrix in the as-quenched condition, and the reverse result is obtained for the aluminum content. Therefore, it is suggested that the increase of the chromium content in the Fe–Al–Mn–Cr alloys would pronouncedly expand the α -Mn field region.

Additionally, as the two present alloys were aged at lower temperature of 350 °C, the diffusion of Mn atom was severely retarded and the formation of the α -Mn became very difficult. Since grain boundaries acted as a more effective preferential diffusion path for Mn atoms than the ferrite grain interior, the precipitation of α -Mn occurred first along grain boundaries by heterogeneous nucleation and then proceeded toward the ferrite grains interior after long-time aging at 350 °C. Since the diffusion rate of Mn atom is sensitive to temperature change, the precipitation of α -Mn became rapid at higher temperatures (i.e. 450, 550 °C), as mentioned above. Nevertheless, it is reasonable to predict that with raising aging temperature to 550 °C, the solubility of aluminum in the ferrite matrix increases in the 10Cr alloy. This inhibits the formation of the Al-rich DO₃ phase within the ferrite matrix during the early stage of

isothermal aging at 550 °C. But along with the precipitation of Mn-rich α -Mn, the surrounding matrix of the α -Mn would be enriched in aluminum, which would enhance the precipitation of Al-rich DO₃ phase in the vicinity of the α -Mn. Also, the amount of the DO₃ phase is gradually less with increasing aging temperature, which is consistent with our experimental results. Therefore, it is proposed that the addition of chromium to the Fe–Al–Mn alloys would enhance the formations of both the α -Mn and the DO₃ phases. This feature has never been found by other workers before.

4. Conclusions

1. When the present alloys were aged at temperatures ranging from 350 to 1050 °C, the phase transformation sequence within the ferrite grains was found to be (α + DO₃ + α -Mn) → (α + α -Mn) → (α + β -Mn) → α .
2. Increasing chromium content in the Fe–Al–Mn–Cr alloys would enhance the formations of both the α -Mn and the DO₃ phases and expand both phase-field regions.

Acknowledgements

The author is pleased to acknowledge the financial support of this research by the National Science Council, Republic of China under Grant NSC91-2216-E-009-019.

References

- [1] Banerji SK. *Met Prog* 1978;(Apr.):59.
- [2] Leavenworth Jr HW, Benz JC. *J Met* 1985;(March):36.
- [3] Charles J, Bergehezan A, Lutts A, Dancoisne PL. *Met Prog* 1981;(May):71.
- [4] Liu TF, Wan CM. *Scripta Metall* 1989;23:1243.
- [5] Zhu XM, Zhang YS. *Corrosion* 1999;55:1.
- [6] Wittmann R, Spindler S, Fischer B, Wagner H, Gerthsen D. *J Mater Sci* 1999;34:1791.
- [7] Prakash U, Buckley RA, Jones H, Greenwood GW. *Philos Mag A* 1992;65:1407.
- [8] Liu TF, Wan CM. *Scripta Metall* 1985;19(7):805.
- [9] Liu TF, Wan CM. *Scripta Metall* 1985;19(6):727.
- [10] Liu TF, Wan CM. *Scripta Metall* 1989;23(7):1087.